RSC Advances

PAPER

View Article Online
View Journal | View Issue

Cite this: *RSC Adv.*, 2017, **7**, 23896

Equilibrium, kinetic and thermodynamic studies of acid soluble lignin adsorption from rice straw hydrolysate by a self-synthesized macro/mesoporous resin

Qianlin Huang,[abd] Xiaoqing Lin,[abce] Lian Xiong,[abc] Chao Huang,[abc] Hairong Zhang,[abc] Mutan Luo,[abd] Lanlan Tian[abd] and Xinde Chen *[abc]

A self-synthesized HQ-8 resin was prepared using a O/W suspension polymerization technique and employed as a potential adsorbent for the removal of acid soluble lignin (ASL) from rice straw hydrolysate (RSH). The structure and morphology of the HQ-8 resin before and after the adsorption of ASL were characterized by Fourier transform infrared spectroscopy (FT-IR), scanning electron microscopy (SEM) and nitrogen adsorption–desorption isotherms. A series of adsorption conditions such as pH value, adsorbent dose, initial concentration, and temperature were systematically investigated to obtain the optimum process parameters. Within the studied range of ASL concentrations, the adsorption equilibrium was found to follow the Freundlich isotherm model well, with R^2 > 0.988. The rate of ASL adsorption onto the HQ-8 resin was very quick, and equilibrium was reached within 50 min of contact. Furthermore, the maximum adsorption capacity of ASL on the HQ-8 resin was 64.61 mg g^{-1} at 298 K at an initial solution pH of 1. The regression results revealed that the ASL adsorption kinetics was represented accurately by a pseudo-second-order model. The efficiency of the HQ-8 resin for the spontaneous and exothermic adsorption of ASL is attributed to the hydrophobic interaction between the cross-linked benzene ring of the HQ-8 resin and the aromatic ring of ASL. In addition, the activation energy of ASL adsorption onto the HQ-8 resin was 35.99 kJ mol^{-1}. In summary, the present adsorption studies of ASL from RSH revealed the potential of a self-synthesized HQ-8 resin to be applied as an alternative adsorbent for lignocellulose hydrolysate detoxification.

Received 24th January 2017
Accepted 24th April 2017

DOI: 10.1039/c7ra01058c

rsc.li/rsc-advances

1. Introduction

Growing concerns over environmental pollution and the depletion of fossil resources have spurred global interest in searching for an alternative source of energy from a renewable source to produce fuels and high value-added chemicals.[1,2] In recent years, lignocellulose agricultural waste has become a potential carbon source to generate biofuels, because it possesses characteristics of abundance, low cost and high sugar content, and it also does not compete with human food resources.[3–5] In China, rice straw is one of the most abundant agricultural wastes and is often abandoned in fields or burned, resulting in a huge waste of resources and serious environmental pollution.[6] A better approach to deal with rice straw is to convert them into biofuels by pretreatment, hydrolysis and fermentation techniques.

To date, several hydrolysis methods in terms of chemical hydrolysis, dilute acid hydrolysis, concentrated acid hydrolysis, enzymatic hydrolysis, as well as ionic liquid were applied to convert lignocellulose materials to simple sugars.[7] Among these methods, dilute acid hydrolysis is the most commonly applied method for producing sugars from lignocellulose in industrial application due to it has lower cost and faster hydrolysis rate than enzyme hydrolysis.[8] However, dilute acid hydrolysis of lignocellulose materials not only produces fermentable reducing sugars but also generates a series of toxic compounds, such as lignin degradation products, and compounds derived from lignocellulose structure, which are toxic to the fermentation microorganisms and strongly interfere with fermentation efficiency.[9–11] Compared with other inhibitors, acid soluble

[a]Guangzhou Institute of Energy Conversion, Chinese Academy of Sciences, No. 2 Nengyuan Road, Tianhe District, Guangzhou 510640, People's Republic of China. E-mail: cxd_cxd@hotmail.com
[b]Key Laboratory of Renewable Energy, Chinese Academy of Sciences, No. 2 Nengyuan Road, Tianhe District, Guangzhou, 510640, People's Republic of China
[c]Guangdong Provincial Key Laboratory of New and Renewable Energy Research and Development, No. 2 Nengyuan Road, Tianhe District, Guangzhou 510640, People's Republic of China
[d]University of Chinese Academy of Sciences, No. 19 Yuquan Road, Beijing 100049, People's Republic of China
[e]Faculty of Chemical Engineering and Light Industry, Guangdong University of Technology, No. 100 Waihuan Xi Road, Panyu District, Guangzhou 510006, People's Republic of China

lignin (ASL) mostly as phenolic compounds of low molar mass has stronger toxic effect on microorganisms and remains in the hydrolysate.[12–14] Furthermore, rice straws possess high lignin content,[15] therefore, rice straw hydrolysate need to be detoxificated to remove ASL before fermentation.

Recently, different detoxification methods and technologies have been used for removal of ASL from actual biomass hydrolysate, including overliming,[16] bio-flocculants,[17] electrochemical[18] and adsorption.[19–21] Among these methods, adsorption has received major concern due to the significant advantages such as low cost, environmentally friendly, high efficiency and energy-saving. Generally, activated carbon, anion-exchange resin and adsorption resin are commonly adsorbents have been used for remove of phenolic compounds from aqueous solution or actual biomass hydrolysate.[19–21] However, detoxification biomass hydrolysate by activated carbon for industrial scale application is limited due to its relatively expensive, low selectivity and difficult regeneration and reuse. Although ion-exchange adsorption is regarded as an effective method for phenolic compounds removal, the most prominent shortcoming is that it is inevitable to use a large amount of acid and alkali in the pretreatment and desorption processes, which increases the cost of separation and produces significant amounts of acid and alkali wastewaters.

Adsorption resins have drawn considerable attention for potential application in separation due to its unique structure and extraordinary adsorption properties.[22] Until present time, only one published work has specifically focused on ASL removal from biomass hydrolysate using adsorption resin.[19] However, the adsorption equilibrium and kinetics of ASL were not investigated. In this work, a novel macro/mesoporous adsorption resin was developed and used to remove ASL from rice straw hydrolysate. The structure and morphology of HQ-8 resin before and after the adsorption of ASL was characterized by Fourier transform infrared (FT-IR) spectroscopy, scanning electron microscopy (SEM) and nitrogen adsorption–desorption isotherms. The adsorption conditions such as pH value, adsorbent dose, initial concentration and temperature were investigated in detail. The adsorption isotherms, kinetics and thermodynamics of ASL onto HQ-8 resin were also discussed systematically.

2. Material and methods

2.1. Materials

Styrene (St), benzoyl peroxide (BPO), poly vinyl alcohol (PVA) (87–89% hydrolyzed, average M_w 124–186 kg mol^{-1}), toluene, methylene blue and liquid paraffin were purchased from Sinopharm Chemical Reagent Co., Ltd., China. Divinyl benzene (63% mixture of isomers remaining ethyl vinyl benzene) was purchased from ZiAn Chemical Co., Ltd., Jinan, China. All materials used in the present study without further purification.

Rice straw was collected from local farmer (Huaian, China). The crude composition of rice straw has been reported to be moisture: 15–18%; cellulose: 41%; hemicellulose: 30%; lignin: 16%; ashes: 10–13%. The rice straw hydrolysate was kindly supplied by Zhongke New Energy Technology Co., Ltd., Huaian, China.

2.2. Methods

2.2.1 Synthesis of HQ-8 resin. HQ-8 resin was synthesized by O/W suspension polymerization technique. Aqueous solution (240 g) containing 0.6 g PVA (0.25 wt%) and few drops 1% methylene blue was transferred into a three-necked round-bottomed flask equipped with a thermometer, a mechanical stirrer, and a reflux condenser, and then was heated to 323 K. Organic solution containing 0.4 g BPO, 40 g monomers ($m_{St} : m_{DVB} = 1 : 1$), and 40 g pore-forming agent ($m_{toluene} : m_{liquid\ paraffin} = 1 : 1$) was added into the flask, and then nitrogen was bubbled through the mixture for 10 min. The mixture was stirred to form a suspension of oil beads with a suitable size in an aqueous solution and then gradually heated to 353 K within 3 h. The reaction was maintained stirred at 353 K for approximately 5 h. After copolymerization, the copolymer beads were filtered out and washed with a large amount of hot water three times, then packed in a fixed-bed column and eluted with anhydrous ethanol until the eluant is transparent when mixed with water. The resins were extracted with ethanol for 24 h in a Soxhlet to remove pore-forming agent and residual monomers, and then were washed with de-ionized water and anhydrous ethanol three times, respectively, to ensure complete removal of impurities. Finally, the resins were dried under vacuum at 333 K for 10 h.

2.2.2 Characterization. The shape and surface morphology of HQ-8 resin before and after the adsorption of ASL was observed by a Hitachi SU70 scanning electron microscope (Hitachi, Japan) operated at 2.0 kV and 10 μA. The specific surface area, pore diameter distribution and pore volume of HQ-8 resin were determined by nitrogen adsorption–desorption isotherms at 77 K using an ASIQMO002-2 analyzer (Quantachrome, USA). Prior to the measurement, the adsorbent (~80 mg) was outgassed at 363 K for 15 h to remove the adsorbed gases and other impurities. The Fourier transform infrared (FT-IR) spectroscopy of the resin was collected on a TENSOR27 (Germany) Fourier transformed infrared instrument using KBr disks.

2.2.3 Effect of initial solution pH on ASL uptake. The effect of solution pH on the adsorption of ASL onto HQ-8 resin was investigated by equilibrating the adsorption mixture with the resin and rice straw hydrolysate at different pH values between 1 and 7. Static adsorption test was performed using 100 mL Erlenmeyer flasks containing 1.0 g of resin and 50 mL hydrolysate. The conical flasks were then shaken at 160 rpm in a thermostatic shaker for 3 h at 298 K. After equilibrium, the liquid phase was sampled with a syringe equipped with the Whatman Spartan 30/0.45 RC syringe filter (0.45 μm) to remove suspended solids. The residual ASL concentration was determined by a UV spectrophotometer, and the adsorption capacity of ASL onto the resin was calculated using the following equation:[23,24]

$$q_e = \frac{(C_0 - C_e)V}{m} \quad (1)$$

2.2.4 Effect of adsorbent dose on the extent of removal of ASL. Different adsorbent doses (0.5, 1.0, 1.5, 2.0, 2.5, 3.0, and 5.0 g) of HQ-8 resin were added into 50 mL hydrolysate in which the concentration of ASL and pH was kept original without any adjustment. The adsorption procedures were the same as described for the effect of pH on ASL uptake.

2.2.5 Adsorption isotherms. 50 mL hydrolysate with different concentrations of ASL (0.83–4.10 g L^{-1}) was contacted with 1.0 g dry resin in 100 mL conical flasks. The flasks were continually shaken in a thermostatic shaker (160 rpm) for 3 h at temperatures of 288, 298, 308 and 318 K, respectively. After equilibrium was reached, the concentrations of ASL in hydrolysate were analyzed by a UV spectrophotometer. The adsorption uptakes of ASL onto the resin were calculated using eqn (1).

2.2.6 Adsorption kinetics. The adsorption kinetics curves of ASL on the HQ-8 resin were performed to evaluate the influence of contact time, at different initial ASL concentrations (0.83, 2.06, and 4.10 g L^{-1}) at various temperatures (288, 298, 318, and 338 K). In the kinetic experiments, 500 mL hydrolysate was contacted with 10 g dry resin in a three-necked flask. Then, the flask was continually shaken in a thermostat water bath with agitation at 160 rpm. Subsequently, the concentration of ASL in the adsorption solution was determined by a UV spectrophotometer at different times until the adsorption equilibrium reached. The amount of ASL on HQ-8 resin at any contact time, t, was calculated as:[25]

$$q_t = \frac{C_0 V_0 - C_t\left(V_0 - \sum_{i=1}^{n} V_i\right)}{m} \quad (2)$$

2.2.7 Reusability evaluation. The regeneration and reusability experiments of HQ-8 resin for ASL was performed using 100 mL Erlenmeyer flasks containing 1.0 g of ASL-loaded resin and 50 mL 95% ethanol in a thermostatic shaker (160 rpm) for 3 h at room temperature. The resins were then filtered and washed with deionized water, allowed to dry and subsequently applied for another adsorption process. The adsorption and desorption procedure was repeated several times.

2.2.8 Analytical methods. The concentrations of ASL in the rice straw hydrolysate were analyzed using the National Renewable Energy Laboratory (NREL) analytical procedures.[26] The sugar concentrations (D-xylose, L-arabinose and D-glucose) in the rice straw hydrolysate were measured by high performance liquid chromatography (HPLC) as previously described.[27]

All the adsorption experiments in this study were carried out at least three times to ensure repeatability.

3. Results and discussion

3.1. Characterization

A FT-IR spectrum was performed to characterize the structure of the HQ-8 resin. For the spectrum of the unloaded resin HQ-8 (Fig. 1(a)), the adsorption peaks appearing at 3082 cm^{-1}, 3057 cm^{-1} and 3038 cm^{-1} were due to the asymmetric and symmetric stretching vibration of C–H bond of the benzene ring. The adsorption peaks at 1604 cm^{-1} and 1488 cm^{-1} were further evidenced presence benzene ring. The asymmetric and symmetric stretching vibration of CH_2 (CH_3) is confirmed by the presence of peaks at 2920 cm^{-1} and 2854 cm^{-1}. In addition, the presence of C=C group is identified by the presence of peaks at 1604 cm^{-1}, 1498 cm^{-1} and 1446 cm^{-1}. The IR spectrum of the HQ-8 resin after loading with ASL (Fig. 1(b)) displays a new strong band at 3442 cm^{-1} is attributed to the presence of –OH due to the fact that the ASL in the hydrolysates largely as phenolic compounds of low molar mass.

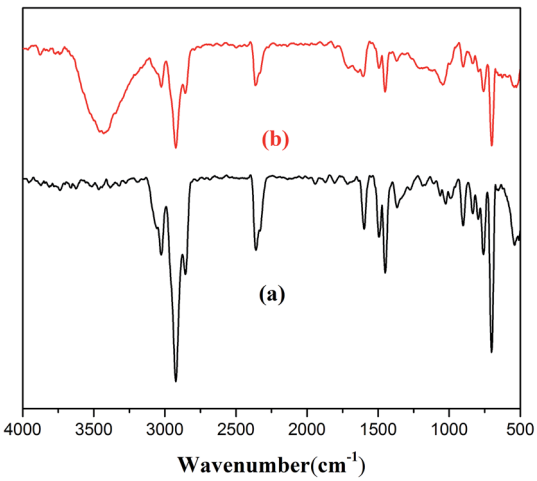

Fig. 1 FT-IR spectrum of (a) HQ-8 resin (b) HQ-8 resin loaded with ASL.

The morphology and surface of HQ-8 resin was observed by SEM, which are demonstrated in Fig. 2(A) and (C). As it depicted, the HQ-8 resin had a spherical form, a rough internal surface and a large number of macropores and mesopores. As showed in Fig. 2(E), the shape of the N_2 adsorption–desorption isotherm curves of the HQ-8 resin seem to close to type IV. A well-defined capillary condensation step occurred between the P/P_0 of 0.05–0.90 with a H1-type hysteresis loop, suggested that the material possesses a uniform mesoporous structure. Moreover, the visible hysteresis loop of desorption isotherm with a relative pressure (P/P_0) over 0.90 indicated that HQ-8 resin had a structure of macropores.[28] These analyses were in accordance with the pore diameter distribution in Fig. 2(F). Furthermore, it can be seen from Fig. 2(F) that the mesoporous are the main pores for HQ-8 resin and the average pore diameter is 32 nm. The HQ-8 resins loaded with ASL were examined using SEM for morphological structure investigations. As can be seen in Fig. 2, it is obvious that HQ-8 resin exhibits less porosity in the adsorption reached equilibrium (Fig. 2(D)) than without adsorption (Fig. 2(C)). This conclusion is also confirmed by surface area measurements using nitrogen adsorption–desorption isotherms, which indicate that the BET surface areas of HQ-8 resin before and after the adsorption of ASL are 199.103 and 58.907 m^2 g^{-1}. Textural parameters derived from the nitrogen adsorption–desorption isotherm data are summarized in Table 1. Based on Table 1, it can be concluded that the HQ-8 resin contains a well-developed pore structure and mesopores play a predominant role. The

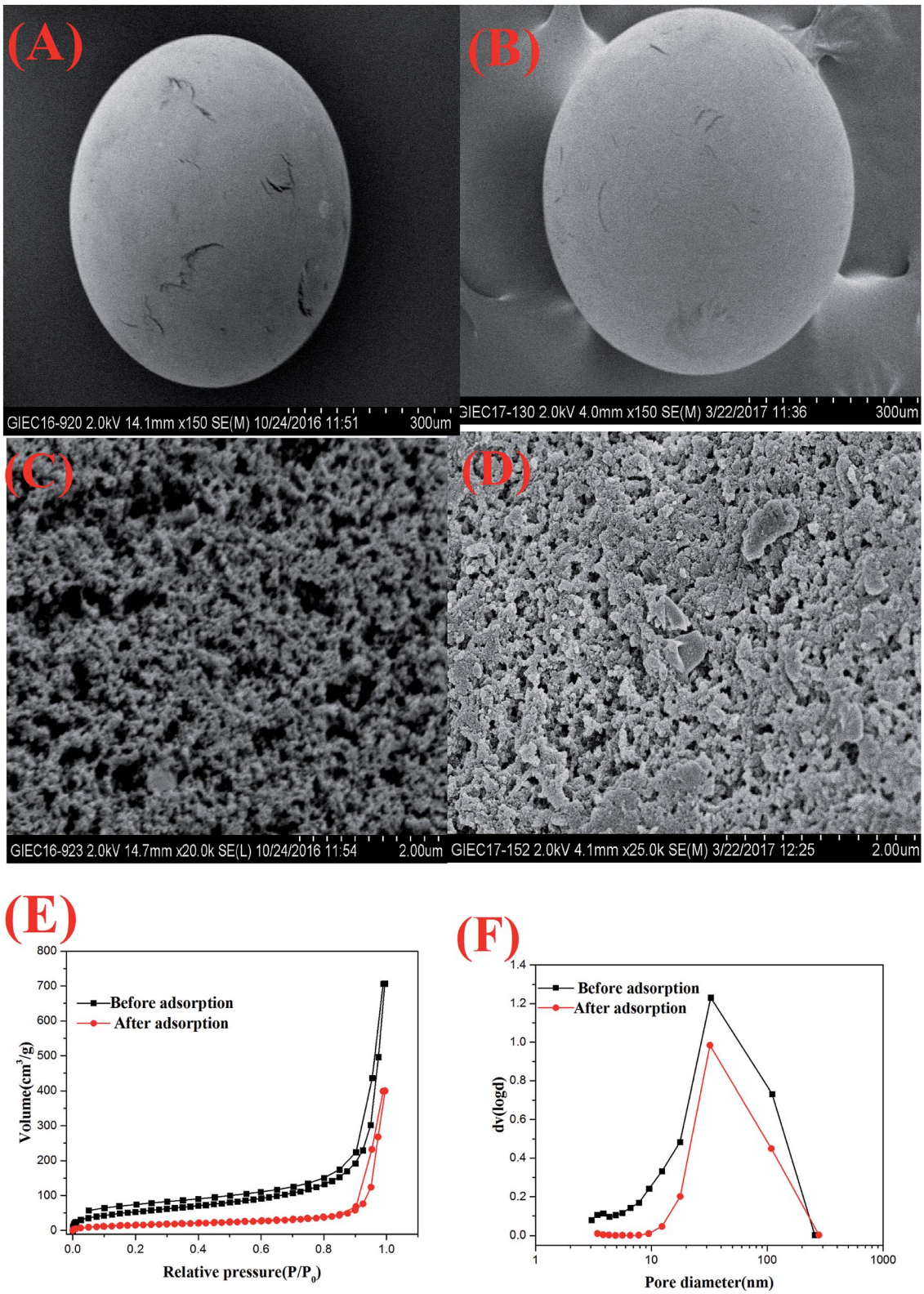

Fig. 2 Characterization of HQ-8 resin: SEM image of (A) (C) HQ-8 resin, (B) (D) HQ-8 resin loaded with ASL; (E) N_2 adsorption–desorption isotherms and (F) pore diameter distribution.

majority of mesopores volume was about 99.44% of the total pore volume, and the mesopore area contributed 75.73% to the total surface area. Besides, when the resin adsorbed the ASL, the textural parameters, such as BET surface area, mesopore area, macropore area, total pore volume, mesopore volume and macropore volume, is obviously decreasing.

Table 1 Physiochemical properties of HQ-8 resin before and after the adsorption of ASL

Resin	Before adsorption	After adsorption
Grain shape	Spherical beads	Spherical beads
Appearance	White	Brown
Structure	Polystyrene divinylbenzene	—
Polarity	Nonpolar	—
Particle size (mm)	0.25–0.85	0.25–0.85
Average pore diameter (nm)	21.965	41.938
BET surface area ($m^2\ g^{-1}$)	199.103	58.907
Mesopore area, S_{meso} ($m^2\ g^{-1}$)	150.784	58.799
Macropore area, S_{macro} ($m^2\ g^{-1}$)	48.319	0.108
Total pore volume ($cm^3\ g^{-1}$)	1.093	0.618
Mesopore volume ($cm^3\ g^{-1}$)	1.036	0.616
Macropore volume ($cm^3\ g^{-1}$)	0.057	0.002

3.2. Effect of the initial solution pH on the sorption

The pH of the initial solution is an important parameter in the adsorption process. In this work, the acid hydrolysate was strongly acidic (pH1) and in order to avoid consuming lots of alkali, the pH was controlled from 1 to 7. Effect of solution pH on the ASL adsorption capacity is presented in Fig. 3. It showed that the ASL adsorption capacity decreased as the pH value increased. When the pH increased from 1 to 7, the ASL adsorption capacity decreased from 66 mg g^{-1} to 49 mg g^{-1}. It seemed that HQ-8 resin could adsorb ASL of the rice straw hydrolysate more efficiently under acidic condition. The most of ASL in the hydrolysate are phenolic compounds of low molar mass.[29] It is inferred that the phenolic compounds had stronger affinity with HQ-8 resin in the acidic solution. It may be attributed to the fact that as the pH value increased, the amount of forming the negative ionic form of phenol is increase.[30] Therefore, all the following experiments were carried out at the initial pH.

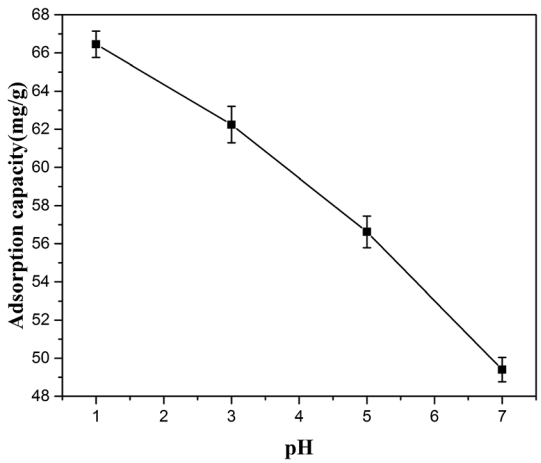

Fig. 3 Effect of pH on the adsorption of ASL on HQ-8 resin.

3.3. Effect of adsorbent dose on the extent of removal of ASL

The selectivity of HQ-8 resin between ASL and sugars is a significantly important parameter in the detoxification process. Selectivity coefficient ($\beta_{ASL/sugar}$) was computed using eqn (3) in order to evaluate the selectivity of HQ-8 resin for ASL compared to sugars.[31]

$$\beta_{ASL/sugar} = D_{ASL}/D_{sugar} \quad (3)$$

Where D_{ASL} and D_{sugar} are the distribution coefficients of ASL and sugars, respectively, which can be expressed as:[32]

$$D = \frac{(C_0 - C_e)V}{C_0 m} \quad (4)$$

The competitive adsorption of ASL in rice straw hydrolysate containing D-xylose, L-arabinose and D-glucose in addition to ASL was examined. The selectivity parameters including distribution and selectivity coefficients are shown in Table 2. As can be seen, the HQ-8 resin exhibits a high distribution coefficient with respect to D-xylose, L-arabinose, D-glucose and total sugar, which indicates the ASL had stronger affinity with HQ-8 resin. Moreover, the selectivity coefficient greater than 1 for each sugar, revealed the high adsorption selectivity between ASL and sugar. It is attributed to the hydrophobic interaction between cross-linked benzene ring of HQ-8 resin and the aromatic ring of ASL.

The effect of adsorbent dose in the range of 0.5–5.0 g on removal of ASL and sugar loss was studied. As shown in Fig. 4, it

Table 2 Selective adsorption of ASL from rice straw hydrolysate by HQ-8 resin

Components	Distribution coefficient ($mL\ g^{-1}$)	Selectivity coefficient
ASL	30.56 ± 0.68	—
D-Xylose	1.39 ± 0.09	22.00 ± 0.97
L-Arabinose	1.57 ± 0.11	19.75 ± 1.51
D-Glucose	1.96 ± 0.09	15.61 ± 0.54
Total sugar	1.51 ± 0.05	20.19 ± 0.53

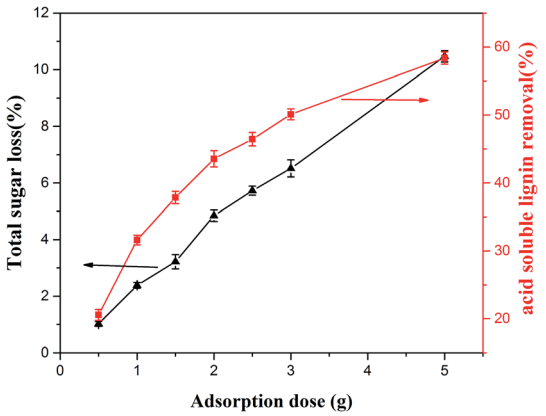

Fig. 4 Effect of adsorbent dose on removal extent of ASL and total sugar loss.

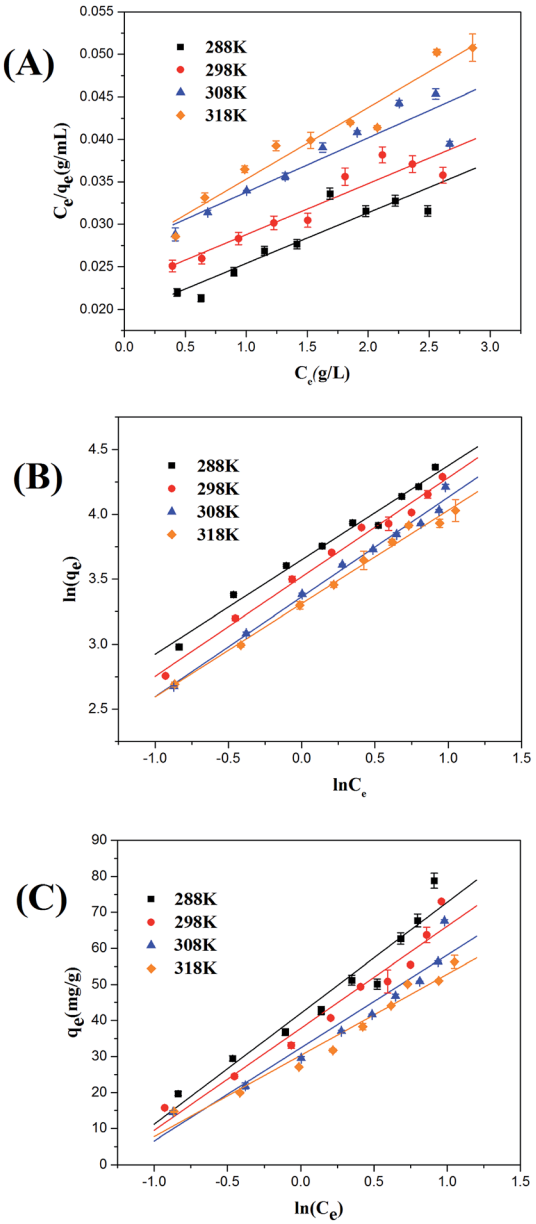

Fig. 5 Langmuir (A), Freundlich (B), and Temkin (C) adsorption isotherms for ASL on HQ-8 resin at different temperatures.

was apparent from the results that the extent of ASL adsorption efficiency increased by increasing the resin amount. This phenomenon was probably due to the fact that the number of available adsorption sites increases with an increase in the resin dose, resulting in an increase in removal efficiency. However, the total sugar lost also increased by increasing the resin amount. Comprehensive consider of the ASL adsorption efficiency and the total sugar loss, 1.0 g dry resin was selected as the most suitable adsorbent dosage in the following experiments.

3.4. Adsorption isotherms

Adsorption isotherm plays a significant role in understanding how adsorbate interacts with adsorbents in the adsorption process. In this study, three commonly used isotherm models, namely Langmuir, Freundlich, and Temkin, were applied to analyze the equilibrium data of sorption of ASL onto HQ-8 resin at 288 to 318 K.

The Langmuir isotherm supposes that a monolayer adsorption occurs onto a special surface containing a finite number of binding sites of uniform strategies of adsorption with no interactions between the molecules adsorbed neither is transmigration on the surface of adsorbent.[33] The linear Langmuir equation is given by:

$$\frac{C_e}{q_e} = \frac{1}{K_L q_m} + \frac{C_e}{q_m} \quad (5)$$

Furthermore, the characteristic parameter of the Langmuir isotherm can be expressed by a dimensionless equilibrium parameter R_L, also known as separation factor defined by Weber and Chakravorti:[34]

$$R_L = \frac{1}{1 + K_L C_0} \quad (6)$$

The value R_L gives an indication of the type of the isotherm and the nature of the adsorption process. It indicates whether the adsorption nature is either unfavorable ($R_L > 1$), linear ($R_L = 1$), favorable ($0 < R_L < 1$) or irreversible ($R_L = 0$).

Different from Langmuir isotherm model, the Freundlich isotherm model is an empirical expression, which is based on the assumption that a multilayer adsorption takes place at the heterogeneous surface and considering the interactions between the adsorbed molecules.[35] The logarithmic form of Freundlich isotherm model can be expressed as:

$$\ln q_e = \ln K_F + \frac{1}{n} \ln C_e \quad (7)$$

K_F and n are the Freundlich constants that can be related to adsorption capacity and adsorption strength, respectively. The n value gives an indication of the favorability of the adsorption process. A value of $1/n < 1$ indicates a favorable adsorption, while $1/n > 1$ indicates a cooperative adsorption.[36]

The Temkin model assumes that a linear decrease in the energy of adsorption with surface coverage and considering the interaction between adsorbate and adsorbent.[37] The Temkin isotherm model is defined as:

$$q_e = \frac{RT}{b_T} \ln K_T + \frac{RT}{b_T} \ln C_e \quad (8)$$

The Langmuir, Freundlich and Temkin equations were used for curve fitting by Origin 8.5, and the parameters of the three equations were summarized and listed in Table 3. By comparing the correlation coefficient (R^2), the Freundlich isotherm model gives the best fit for the adsorption of ASL onto HQ-8 resin. All $1/n$ values obtained from the Freundlich isotherm mode at different temperatures less than 1, indicating the adsorption was favorable. As seen from Table 3, the calculated R_L values at all three temperatures were between 0 and 1, indicating the adsorption of ASL onto HQ-8 resin was favorable. However, the

Table 3 Isotherm parameters of each isotherm model for the sorption of ASL onto HQ-8 resin at different temperatures

	Langmuir isotherm				Freundlich isotherm			Temkin isotherm		
T (K)	q_m (mg g^{-1})	K_L (L g^{-1})	R_L (g L^{-1})	R^2	$1/n$	K_F (mg g^{-1}) (L g^{-1})$^{1/n}$	R^2	K_T (L g^{-1})	b_T (J mol^{-1})	R^2
288	167.5	0.31	0.44	0.8148	0.727	38.47	0.9820	3.91	77.76	0.9394
298	166.4	0.26	0.48	0.8796	0.766	33.72	0.9883	2.11	87.55	0.9462
308	153.0	0.23	0.51	0.8274	0.769	28.81	0.9895	2.21	99.32	0.9218
318	118.6	0.31	0.44	0.9415	0.719	27.46	0.9912	2.10	117.36	0.9618

low correlation coefficient (R^2) is an indication that it is not only a monolayer adsorption and the equilibrium isotherms cannot be described by Langmuir model. It can also be observed from Table 3 that the experimental data are not well fitted to the Temkin isotherm model. It can be explained that the interaction between adsorbate and adsorbent, and the adsorption process is simply a function of surface coverage.

3.5. Thermodynamic studies

The thermodynamic parameters ΔG° (standard free energy), ΔH° (enthalpy change) and ΔS° (entropy change) were calculated to determine the inherent energy change of adsorbent after adsorption and the mechanism involved in adsorption process. The thermodynamic parameters of ΔH° and ΔS° can be obtained respectively from the slope and intercept of ln K_C *versus* $1/T$ in Fig. 6(A), by using the linear Van's Hoff equation:[38]

$$\ln K_C = \frac{\Delta S^\circ}{R} - \frac{\Delta H}{RT} \quad (9)$$

$$K_C = \frac{q_e}{C_e} \quad (10)$$

The ΔG° was calculated by the follow equation:

$$\Delta G^\circ = \Delta H^\circ - T\Delta S^\circ \quad (11)$$

As is shown in Table 4, ΔG° was negative value, indicating that the adsorption process was spontaneous at all temperatures. Furthermore, the increase in ΔG° value with increasing temperature indicates that adsorption of ASL onto HQ-8 resin becomes favorable at a lower temperature. The negative value of ΔH° indicates that the sorption process of ASL on HQ-8 resin was exothermic in nature.[25] The adsorption capacity of ASL onto HQ-8 resin decreased with increasing of temperature. In addition, the absolute values less than 20 kJ mol^{-1} implied that the adsorption was a physical process.[39] The negative value of ΔS° showed that more ordered arrangement of ASL was shaped on HQ-8 resin surface after adsorption.

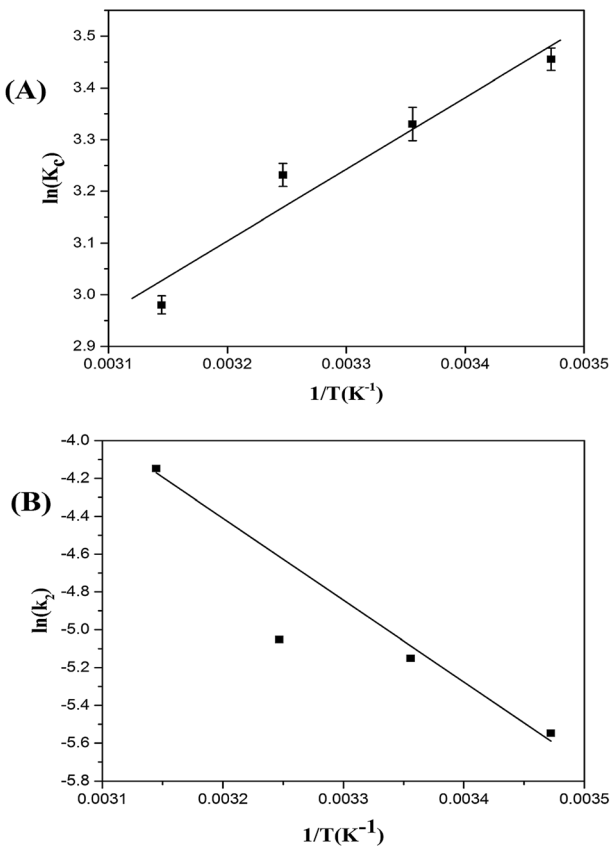

Fig. 6 Plot of ln K_C *versus* $1/T$ (A) plot of ln k_2 *versus* $1/T$ (Arrhenius plot) (B) for ASL adsorption on HQ-8 resin.

3.6. Kinetics studies

3.6.1 Effect of solution temperature on ASL adsorption. Effect of solution temperature on the ASL adsorption capacity is shown in Fig. 7(A), the adsorption capacity of ASL onto HQ-8 resin was found to decrease slightly with the increase in solution temperature from 288 K to 318 K, indicating the exothermic nature of the sorption reaction. This result consistent with the adsorption equilibrium results (Fig. 5(A–C)) and the adsorption thermodynamic analysis discussed above. The equilibrium time decreased from 50 to 10 min

Table 4 Thermodynamic parameters for the sorption of ASL onto HQ-8 resin at different temperatures

T (K)	ΔG° (kJ mol^{-1})	ΔH° (kJ mol^{-1})	ΔS° (J mol^{-1} K^{-1})
288	−8.34	−11.53	−11.08
298	−8.23		
308	−8.13		
318	−8.01		

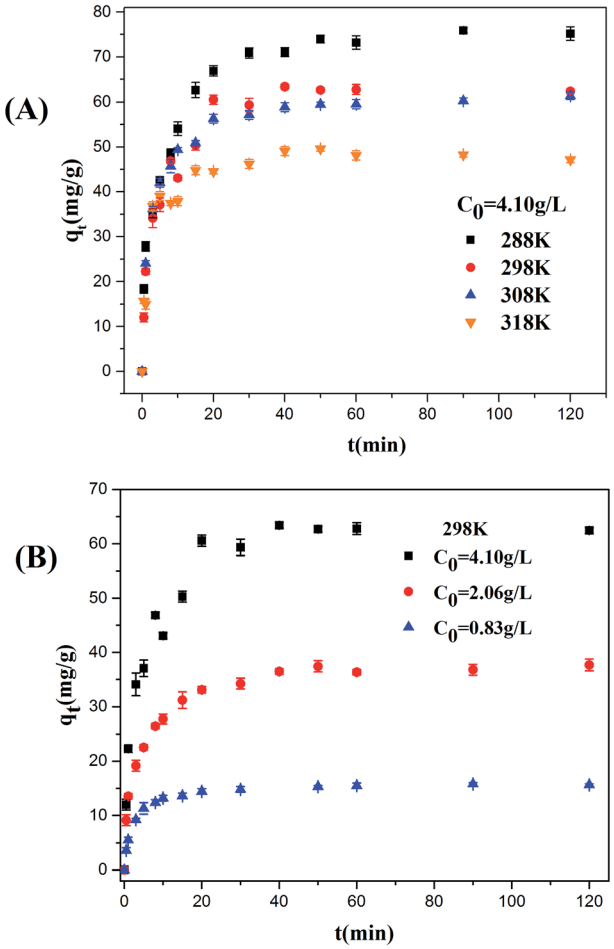

Fig. 7 The effect of contact time on the sorption of ASL onto HQ-8 resin at various temperatures (A); different initial concentrations of ASL (B).

with increasing temperature from 288 to 318 K. These results probably due to the increase in diffusion rate of ASL with increasing temperature. Besides, the adsorption rate of ASL onto HQ-8 resin was fast in the first stages of the contact period at all experiment temperature, and then it became slower near the equilibrium. It may be attributed to the fact that as the contact time increased, the adsorption sites were obtained will became more difficult due to repulsive forces between the solute molecules on the solid and bulk phases.

3.6.2 Effect of initial concentration on ASL adsorption. The effect of initial ASL concentration on the adsorption time and adsorption rate was investigated. As shown in Fig. 7(B), the sorption capacity of at equilibrium increase from 15 to 64 mg g^{-1} with initial concentration from 0.83 to 4.10 g L^{-1}. This phenomenon may be explained by the saturation of accessible-adsorbent sites of adsorbents. The equilibrium time decreased from 40 to 20 min when increasing ASL initial concentration from 0.83 to 4.10 g L^{-1} at 298 K. This was attributed to the fact that the mass transfer driving force increased with increasing initial concentration, which caused faster equilibrium.

3.6.3 Adsorption kinetics. The adsorption kinetics is useful to determine the rate of the adsorption and examine the controlling mechanism of the adsorption process. In this work, the Lagergren's pseudo first-order and pseudo second-order models were adopted to investigate the adsorption kinetic behavior of ASL onto HQ-8 resin.

The equation for Lagergren's pseudo-first order kinetics is presented as follows:[40]

$$\ln(q_e - q_t) = \ln q_e - k_1 t \quad (12)$$

The values of k_1 and adsorption capacity q_e are computed from the plots of $\ln(q_e - q_t)$ *versus* t (Fig. 8(A) and 9(A)) and showed in Table 5. Comparing the experimental obtained equilibrium adsorption ($q_{e,exp}$) with the calculated results ($q_{e,cal}$), it is obvious that there is no agreement between the values. The correlation coefficients (R^2) for the first model show poor linearity. Therefore, the adsorption deviates from the Lagergren's pseudo-first model.

The pseudo-second-order kinetic model is expressed as follows:[41]

$$\frac{t}{q_t} = \frac{1}{k_2 q_e^2} + \frac{t}{q_e} \quad (13)$$

k_2 is the pseudo-first-order rate constant for the sorption is obtained by a plot of t/q_t against t (Fig. 8(A) and 9(A)). It can be observed from Table 5 that the values of the correlation coefficients ($R^2 > 0.99$) for all the operating condition indicate that the adsorption process follows pseudo-second order kinetic model. Meanwhile, this conclusion is also supported by the comparisons between the experimental results ($q_{e,exp}$) and model predictions ($q_{e,cal}$).

To better understand the adsorption mechanism of ASL onto HQ-8 resin, the rate limiting step was estimated by the Weber and Morris intraparticle diffusion model.[42,43] The linear form of this equation is:

$$q_t = k_i t^{0.5} + C \quad (14)$$

Adsorption kinetics may be controlled by the rate limiting step of the process and the adsorption mechanism. Generally, if the plot of q_t *versus* $t^{0.5}$ yields a straight line, the adsorption process is controlled by intra-particle diffusion; and if the data exhibit multi-linear plot, the adsorption process is influenced by two or more stages.[44] Fig. 8(C) and 9(C) show that the plot of q_t *versus* $t^{0.5}$ is multi-linear. Clearly, there are three linear portions to explain the adsorption stages, the first stage is attributed to the instantaneous adsorption or external surface adsorption, the second to intraparticle diffusion and the third portion referred to the final equilibrium stage for which the intraparticle diffusion started to slow down due to the extremely low adsorbate concentration left in the solution.[45] Fig. 8(C) and 9(C) also showed the linear lines of the second and the third stages did not pass through the origin, indicating that intra-particle diffusion is not the only rate-limiting.[46,47] The intra-particle diffusion constant values are shown in Table 5.

3.7. Adsorption activation energy

The activation energy of adsorption, E_a (kJ mol^{-1}), is calculated from the second order rate constant (k_2) obtained from the pseudo-second order kinetic model using the Arrhenius equation:

$$\ln k_2 = -\frac{E_a}{RT} + A \quad (15)$$

The apparent activation energy E_a gives an indication of the type of the adsorption process, physical or chemical. The Arrhenius plot of ln k_2 *versus* $1/T$ for the sorption of ASL on the resin is presented in Fig. 6(B). The calculated activation energy E_a was 35.99 kJ mol^{-1} (ranging between 5 and 40 kJ mol^{-1}), revealing physical nature of the adsorption process.[48,49] This finding was consistent with the thermodynamic results.

3.8. Reusability

The regeneration and reuse of the resin is significance in term of economic cost. It was found that the HQ-8 resin could be well desorbed by 95% ethanol at room temperature. Fig. 10 shows the ASL adsorption capacity in five adsorption–desorption cycles. It can be seen that the resin exhibited good reusability with almost

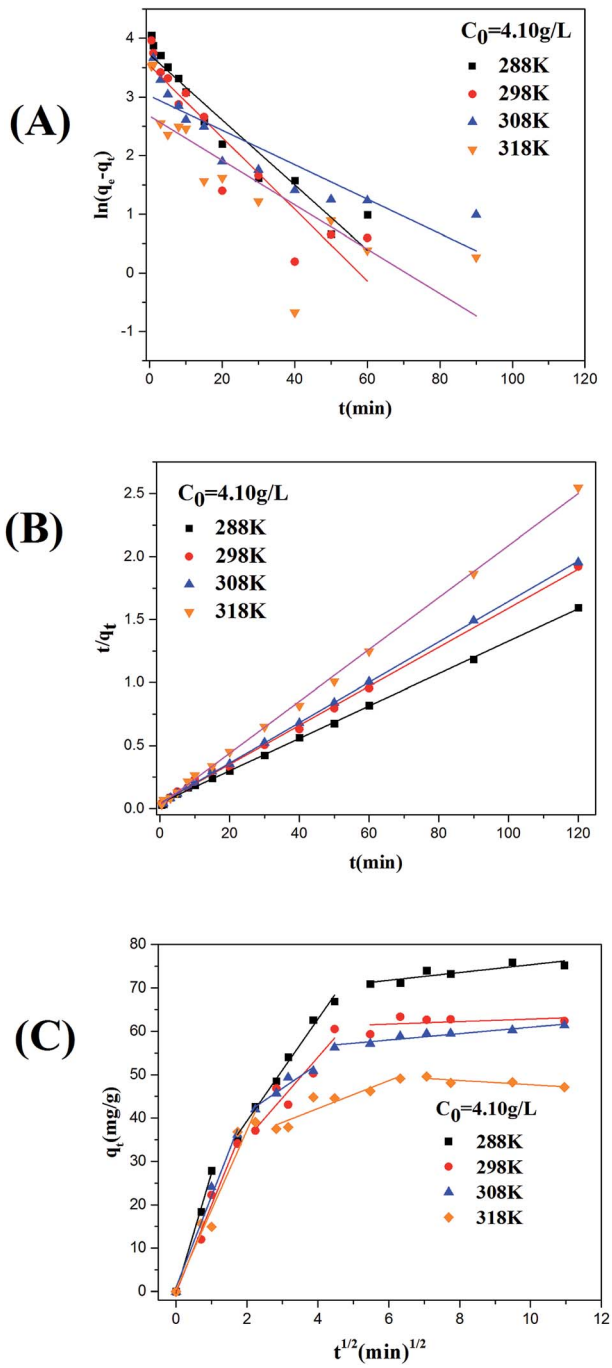

Fig. 8 Pseudo-first-order (A), pseudo-second-order (B), and intra-particle diffusion (C) kinetic models for batch adsorption of ASL by HQ-8 resin at different temperatures.

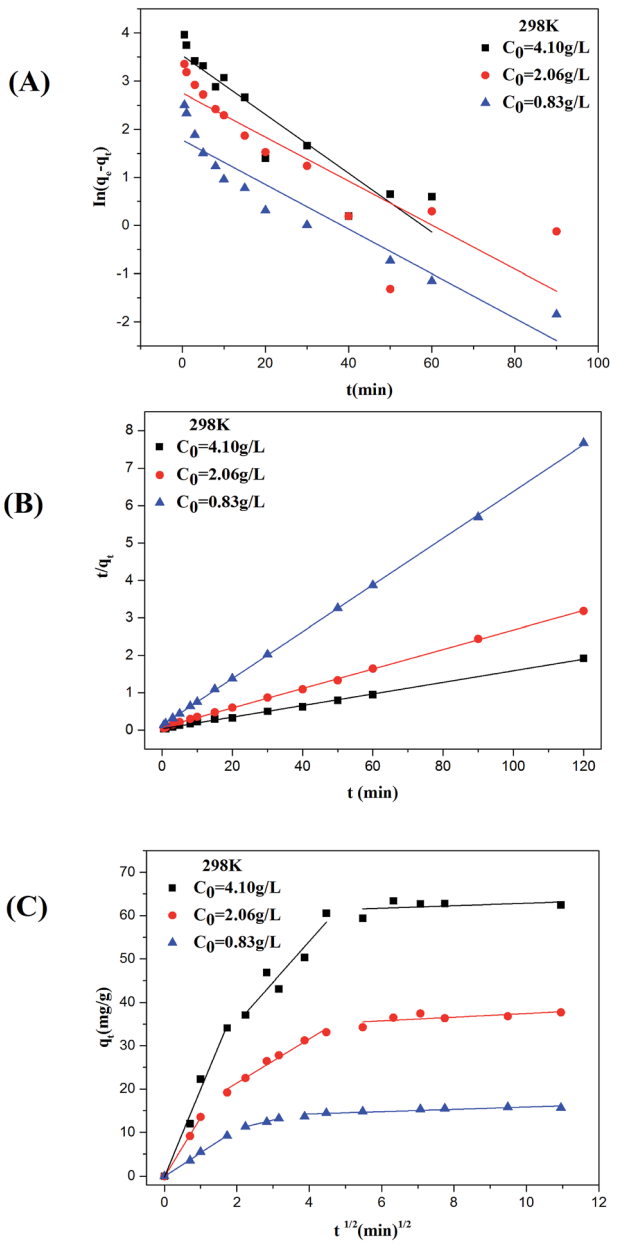

Fig. 9 Pseudo-first-order (A), pseudo-second-order (B), and intra-particle diffusion (C) kinetic models for batch sorption of ASL by HQ-8 resin at different initial concentrations.

Table 5 Kinetic constant parameters obtained for acid soluble lignin on HQ-8 resin

			Pseudo-first order			Pseudo-second order			Intraparticle diffusion model		
T (K)	C_0 (g L^{-1})	$q_{e,exp}$ (mg g^{-1})	k_1 (min^{-1})	$q_{e,cal}$ (mg g^{-1})	R^2	k_2 (g mg^{-1} min^{-1})	$q_{e,cal}$ (mg g^{-1})	R^2	k_i (mg g^{-1} min^{-1})	C (mg g^{-1})	R^2
288	4.10	75.94	0.0555	41.20	0.919	0.0039	77.76	0.9992	11.8	15.75	0.9887
298	0.83	15.81	0.0463	5.92	0.893	0.0291	16.01	0.9999	2.0	6.73	0.9870
298	2.06	37.71	0.0457	15.67	0.729	0.0088	38.46	0.9994	5.1	11.17	0.9769
298	4.10	64.61	0.0611	34.17	0.856	0.0058	64.56	0.9984	9.4	16.41	0.8473
308	4.10	62.21	0.0294	20.51	0.788	0.0064	62.34	0.9998	5.6	30.08	0.8837
318	4.10	49.02	0.0379	14.52	0.635	0.0158	48.52	0.9987	3.2	29.26	0.8374

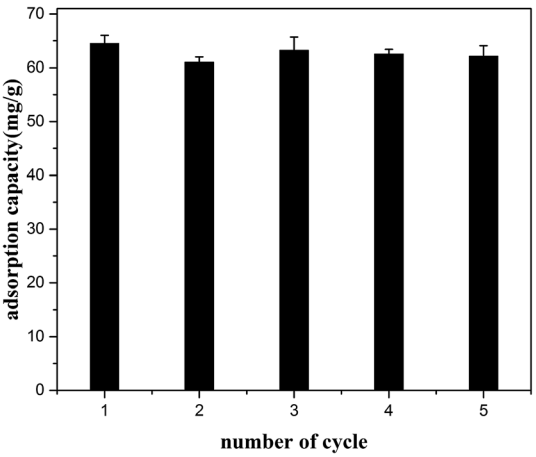

Fig. 10 Effect of the regeneration cycles on the adsorption capacity of ASL on HQ-8 resin at 298 K.

stable efficiency, indicating that HQ-8 resin is a promising valuable adsorbent to remove ASL from the lignocellulose hydrolysate.

4. Conclusion

In the present investigation, a macro/mesoporous resin, HQ-8, was evaluated as a novel adsorbent with high adsorption capacity for removal of ASL. The study of influence of solution pH indicated that the HQ-8 resin exhibited better adsorption performance under acidic conditions. The maximum adsorption amount of ASL onto HQ-8 resin was achieved to 64.61 mg g^{-1} at a pH of 1 at 298 K. The resin dose inversely affected the adsorption capacity of ASL onto HQ-8 resin, whereas the adsorption capacity increased with increasing initial ASL concentration. Within the studied range of ASL concentrations, the adsorption equilibrium was found to follow the Freundlich isotherm model well, with R^2 > 0.988. The adsorption of ASL onto HQ-8 resin reached equilibrium in a short contact time (within 50 min), resulting in fast and efficient ASL removal, which would be beneficial for practical purposes. The regression results revealed that the rate of the ASL adsorption process was found to conform accurately to the pseudo-second-order kinetic model. The efficiency of HQ-8 resin for the spontaneous and exothermic adsorption of ASL is attributed to the hydrophobic interaction between cross-linked benzene ring of HQ-8 resin and the aromatic ring of ASL. In addition, the Arrhenius activation energy of ASL adsorption onto HQ-8 resin is 35.99 kJ mol^{-1}, suggested physical nature of the adsorption process. Thus, the present adsorption study has provided a new, efficient, and stable adsorbent with potential for practical application in the detoxification of lignocellulose hydrolysate.

List of symbols

A	Arrhenius constant
b_T	Temkin constant related to heat of adsorption
C	Intraparticle diffusion model constant (mg g^{-1})
C_0	Initial concentration of ASL in hydrolysate (g L^{-1})
C_e	Equilibrium concentration of ASL in hydrolysate (g L^{-1})
C_t	Concentration of ASL in solution at contact time (g L^{-1})
D	Distribution coefficients (mL g^{-1})
E_a	Apparent activation energy (kJ mol^{-1})
k_1	Pseudo-first-order rate constant (min^{-1})
k_2	Second order rate constant in (mg g^{-1} min^{-1})
k_i	Intraparticle diffusion rate (mg g^{-1} $min^{-1/2}$)
K_C	Thermodynamic equilibrium constant
K_F	Freundlich adsorption isotherm constant (mg g^{-1}) (L $g^{-1})^{1/n}$
K_L	Langmuir constant (L g^{-1})
K_T	Temkin isotherm constant (L g^{-1})
M	Mass of the dry resin (g)
N	Freundlich adsorption isotherm constant
q_e	Equilibrium adsorption capacity (mg g^{-1})
$q_{e,cal}$	Calculate adsorption capacity (mg g^{-1})
$q_{e,exp}$	Experimental adsorption capacity (mg g^{-1})
q_m	Maximum saturated adsorption capacity (mg g^{-1})
q_t	Adsorption capacity of ASL at contact time (mg g^{-1})
R	Gas constant (8.314 J mol^{-1} K^{-1})
R_L	Langmuir equilibrium parameter
T	Contact time (min)
T	Solution temperature (K)
V	Volume of solution (L)
V_0	Initial volume of solution (L)
V_i	Sampling volume (L)
ΔG°	Gibbs free energy change (kJ mol^{-1})
ΔH°	Enthalpy change (kJ mol^{-1})
ΔS°	Entropy change (J mol^{-1} K^{-1})
β	Selectivity coefficient

Acknowledgements

The authors are grateful to the financial support from the Project of National Natural Science Foundation of China (51508547), Pearl River S&T Nova Program of Guangzhou (201710010096), the Science and Technology Planning Project of Guangdong Province, China (2016A010104009), the Project of Huaian Science and Technology (HAS201623), the Foundation of Director of Guangzhou Institute of Energy Conversion, Chinese Academy of Sciences (y407r41001) and the Project of Guangdong Provincial Key Laboratory of New and Renewable Energy Research and Development (Y709jh1001).

References

1 X. Tang, Y. Sun, X. Zeng, W. Hao, L. Lin and S. Liu, *Energy Fuels*, 2014, **28**, 4251–4255.
2 D. T. N. N. Nguyen, M. L. Lameloise, W. Guiga, R. Lewandowski, M. Bouix and C. Fargues, *J. Membr. Sci.*, 2016, **512**, 111–121.
3 C. C. Geddes, I. U. Nieves and L. O. Ingram, *Curr. Opin. Biotechnol.*, 2011, **22**, 312–319.
4 G. W. Huber, S. Iborra and A. Corma, *Chem. Rev.*, 2006, **106**, 4044–4098.
5 X. Lin, Q. Huang, G. Qi, S. Shi, L. Xiong, C. Huang, X. Chen, H. Li and X. Chen, *Sep. Purif. Technol.*, 2017, **174**, 222–231.
6 L. H. Deng, Y. H. Wang, Y. Zhang and R. Y. Ma, *J. Food Biochem.*, 2007, **31**, 195–205.
7 M. Balat, *Energy Convers. Manage.*, 2011, **52**, 858–875.
8 P. Lenihan, A. Orozco, E. O'neill, M. Ahmad, D. Rooney and G. Walker, *Chem. Eng. J.*, 2010, **156**, 395–403.
9 S. Larsson, E. Palmqvist, B. Hahn-Hägerdal, C. Tengborg, K. Stenberg, G. Zacchi and N.-O. Nilvebrant, *Enzyme Microb. Technol.*, 1999, **24**, 151–159.
10 S. I. Mussatto and I. C. Roberto, *Bioresour. Technol.*, 2004, **93**, 1–10.
11 L. J. Jonsson, B. Alriksson and N. O. Nilvebrant, *Biotechnol. Biofuels*, 2013, **6**, 6–16.
12 T. Ezeji, N. Qureshi and H. P. Blaschek, *Biotechnol. Bioeng.*, 2007, **97**, 1460–1469.
13 E. Palmqvist and B. Hahn-Hägerdal, *Bioresour. Technol.*, 2000, **74**, 25–33.
14 Y. Xia, H. H. P. Fang and T. Zhang, *RSC Adv.*, 2013, **3**, 15528–15542.
15 K. S. Yadav, S. Naseeruddin, G. S. Prashanthi, L. Sateesh and L. V. Rao, *Bioresour. Technol.*, 2011, **102**, 6473–6478.
16 R. Purwadi, C. Niklasson and M. J. Taherzadeh, *J. Biotechnol.*, 2004, **114**, 187–198.
17 W. Zhang, X. Zhang, L. Bao and G. Wei, *Chem. Biochem. Eng. Q.*, 2012, **26**, 127–136.
18 K. M. Lee, K. Min, O. Choi, K.-Y. Kim, H. M. Woo, Y. Kim, S. O. Han and Y. Um, *Bioresour. Technol.*, 2015, **187**, 228–234.
19 T. J. Schwartz and M. Lawoko, *BioResources*, 2010, **5**, 2337–2347.
20 Z. Wang, J. Jiang, X. Wang, Y. Fu, Z. Li, F. Zhang and M. Qin, *Bioresour. Technol.*, 2014, **174**, 198–203.
21 H. Miyafuji, H. Danner, M. Neureiter, C. Thomasser, J. Bvochora, O. Szolar and R. Braun, *Enzyme Microb. Technol.*, 2003, **32**, 396–400.
22 C. Detoni, C. H. Gierlich, M. Rose and R. Palkovits, *ACS Sustainable Chem. Eng.*, 2014, **2**, 2407–2415.
23 X. Lin, L. Xiong, C. Huang, X. Yang, H. Guo, X. Chen and X. Chen, *Desalin. Water Treat.*, 2016, **57**, 366–381.
24 X. Lin, J. Wu, J. Fan, W. Qian, X. Zhou, C. Qian, X. Jin, L. Wang, J. Bai and H. Ying, *J. Chem. Technol. Biotechnol.*, 2012, **87**, 924–931.
25 X. Lin, Q. Huang, G. Qi, L. Xiong, C. Huang, X. Chen, H. Li and X. Chen, *Chemosphere*, 2017, **171**, 231–239.
26 A. Sluiter, B. Hames, R. Ruiz, C. Scarlata, J. Sluiter, D. Templeton and D. Crocker, *Laboratory analytical procedure*, 2008, vol. 1617, http://www.nrel.gov/biomass/analyticalprocedures.html.
27 X. Lin, L. Xiong, G. Qi, S. Shi, C. Huang, X. Chen and X. Chen, *ACS Sustainable Chem. Eng.*, 2015, **3**, 702–709.
28 X. Yang, L. Wu, L. Ma, X. Li, T. Wang and S. Liao, *Catal. Commun.*, 2015, **59**, 184–188.
29 S. Yasuda, K. Fukushima and A. Kakehi, *J. Wood Sci.*, 2001, **47**, 69–72.
30 J. H. Huang, *J. Hazard. Mater.*, 2009, **168**, 1028–1034.
31 D. K. Singh and S. Mishra, *Anal. Chim. Acta*, 2009, **644**, 42–47.
32 M. Monier, N. H. Elsayed and D. A. Abdel-Latif, *Polym. Int.*, 2015, **64**, 1465–1474.
33 I. Langmuir, *J. Am. Chem. Soc.*, 1916, **38**, 2221–2295.
34 T. W. Weber and R. K. Chakravorti, *AIChE J.*, 1974, **20**, 228–238.
35 H. Freundlich, *J. Phys. Chem.*, 1906, **57**, 1100–1107.
36 I. Tan, A. Ahmad and B. Hameed, *J. Hazard. Mater.*, 2009, **164**, 473–482.
37 K. K. Choy, G. McKay and J. F. Porter, *Resour., Conserv. Recycl.*, 1999, **27**, 57–71.
38 V. Gupta, P. Singh and N. Rahman, *J. Colloid Interface Sci.*, 2004, **275**, 398–402.
39 X. Zhou, J. Fan, N. Li, W. Qian, X. Lin, J. Wu, J. Xiong, J. Bai and H. Ying, *Ind. Eng. Chem. Res.*, 2011, **50**, 9270–9279.
40 S. Lagergren, *K. Sven. Vetenskapsakad. Handl.*, 1898, **24**, 1–39.
41 Y.-S. Ho and G. McKay, *Process Saf. Environ. Prot.*, 1998, **76**, 183–191.
42 G. Annadurai, R.-S. Juang and D.-J. Lee, *J. Hazard. Mater.*, 2002, **92**, 263–274.
43 S. Srivastava, R. Tyagi and N. Pant, *Water Res.*, 1989, **23**, 1161–1165.
44 C. Long, A. Li, H. Wu and Q. Zhang, *Colloids Surf., A*, 2009, **333**, 150–155.
45 H. Zaghouane-Boudiaf and M. Boutahala, *Chem. Eng. J.*, 2011, **170**, 120–126.
46 F.-C. Wu, R.-L. Tseng and R.-S. Juang, *Environ. Technol.*, 2001, **22**, 205–213.
47 I. Langmuir, *J. Am. Chem. Soc.*, 1918, **40**, 1361–1403.
48 A. Ozcan, A. Ozcan and O. Gok, *Hazardous Materials and Wastewater—Treatment, Removal and Analysis*, Nova Science Publishers, New York, 2007.
49 E. Unuabonah, K. Adebowale and B. Olu-Owolabi, *J. Hazard. Mater.*, 2007, **144**, 386–395.

